

# Synthesis and Spectroscopic Determination of the Coordination Differences of Cadmium and Zinc Complexes of Dehydroacetic Acid with Pyridine and $\gamma$ -Picoline

Erika Martins de Carvalho\*

Instituto de Tecnologia em Fármacos, Farmanguinhos/ FIOCRUZ. Rua Sizenando Nabuco, 100, Manguinhos, 21041-250, Rio de Janeiro, RJ, Brazil

Roselene Ribeiro Riente

Instituto de Tecnologia em Fármacos, Farmanguinhos/ FIOCRUZ. Rua Sizenando Nabuco, 100, Manguinhos, 21041-250, Rio de Janeiro, RJ, Brazil

José Daniel Figueroa Villar

Grupo de Química Medicinal, Departamento de Química, Instituto Militar de Engenharia, Praça General Tibúrcio, 80, Urca, 22290-270, Rio de Janeiro, RJ, Brazil

## Abstract

Various complexes of DHA with transition-metal cations are known for their antifungal properties. Here, four novel Zn and Cd complexes were prepared via the substitution of water by pyridine and  $\gamma$ -picoline using  $\text{Zn}(\text{DHA})_2(\text{H}_2\text{O})_2$  (2) and  $\text{Cd}(\text{DHA})_2(\text{H}_2\text{O})_2$  (3) as starting materials. The products were characterized by IR, UV, elemental analysis, TGA and NMR techniques, including correlation times and intermolecular distance measurements using the NULL pulse sequence. The experimental data were compared to the molecular modeling results using DFT and the semiempirical method PM3, confirming that the pentacoordinated Zn complexes have bipyramidal geometry while the Cd complexes have the expected octahedral geometry. These results show that substitution of Zn by Cd leads to an important modification of the coordination structure, especially when strong ligands are involved.

**Keywords:** Zinc-Cadmium exchange; Coordination geometry difference; Dehydroacetic acid; Bipyramidal geometry; NULL; Molecular modeling.



CC BY: [Creative Commons Attribution License 4.0](https://creativecommons.org/licenses/by/4.0/)

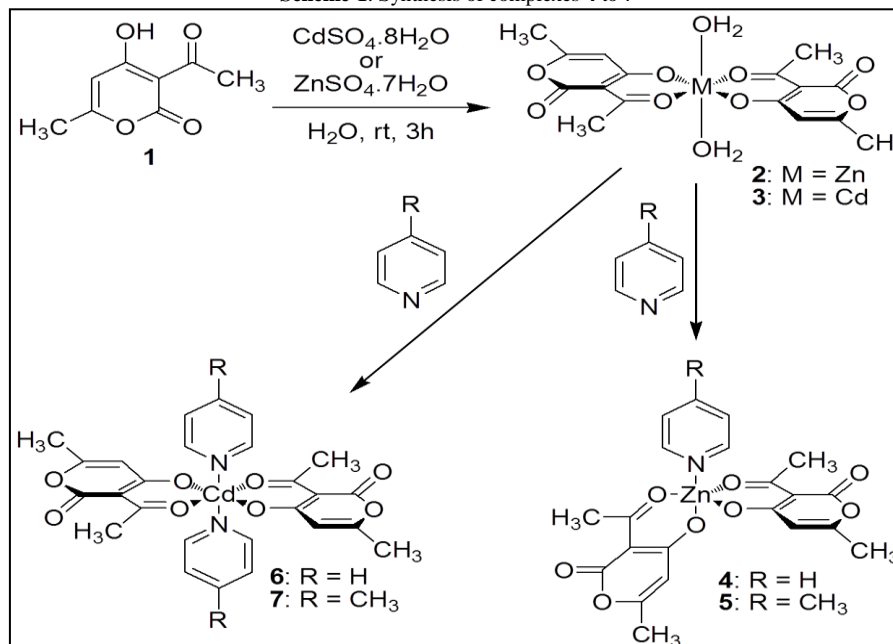
## 1. Introduction

Many studies on complexes of transition metal ions with different ligands have been reported due to their importance in biochemical processes [1-5]. However, complexes of metals from group 12 constitute an especially attractive topic in view of the marked differences among the chemical behavior and biological activity of these metal cations. Zinc is the second-most abundant trace metal in the human body [6-8], and it is essential for the structure of zinc finger proteins and the catalytic action of many enzymes. On the other hand, cadmium, which is environmentally dangerous [9] and widely used in industrial processes, is very toxic. The toxic effect of cadmium is associated with the fact that it often competes with zinc for a variety of important binding sites in cells, including gene regulation [10, 11]. Also, because  $^{67}\text{Zn}$  has a very low natural abundance (4.1%), possesses a low molar receptivity ( $2.9 \times 10^{-3}$  relative to  $^1\text{H}$ ) and a high quadrupolar moment ( $Q = 15.0 \text{ fm}^2$ ), it is difficult to obtain  $^{67}\text{Zn}$  NMR spectra. Because of these properties, the exchange of Zinc for Cadmium has been used in solution and in the solid state to examine the metal complexation environment of zinc-containing biomolecules by  $^{113}\text{Cd}$  NMR [12-14]. On the other hand, it has been shown that Zn substitution for Cd leads to important changes in the coordination geometry of complexes with dehydroacetic acid [13-15].

In a previous work [15], zinc and cadmium complexes were synthesized with dehydroacetic acid (DHA) (1),  $\text{Zn}(\text{DHA})_2(\text{H}_2\text{O})_2$  (2),  $\text{Cd}(\text{DHA})_2(\text{H}_2\text{O})_2$  (3) and their analogues, which were prepared through substitution of the water ligands on complexes 2 and 3 by DMSO. These complexes have been shown to possess modest antifungal properties and coordination geometry differences [16].

In order to determine if stronger ligands would increase the differences between Zn and Cd complexes with DHA, we have prepared novel Zn and Cd complexes through substitution of water by pyridine and  $\gamma$ -picoline in compounds 2 and 3 (Scheme 1). In this work, we have shown that with the involvement of pyridine-type ligands, the differences in coordination geometry of Zn and Cd complexes with DHA are even greater. The structural characterization of these complexes was carried out using detailed NMR methods, including correlation time and intermolecular distance measurements, and they were confirmed by molecular modeling.

Scheme-1. Synthesis of complexes 4 to 7



## 2. Material and Methods

### 2.1. Materials

The following reagents were used to prepare the desired complexes without further treatment or purification: dehydroacetic acid (Merck, analytical reagent),  $\text{ZnSO}_4 \cdot 7\text{H}_2\text{O}$  (Schuchardt),  $\text{CdSO}_4 \cdot 8/3 \text{H}_2\text{O}$  (Reagen) and  $\gamma$ -picoline (Erich). Methanol (Merck, spectroscopic grade) was used as solvent for the UV analysis.

### 2.2. Melting Points, IR, UV, TGA and Elemental Analysis

Melting points were determined using a BUCHI Melting Point B-545 apparatus and are uncorrected. The infrared spectra (IR) were recorded using samples prepared in KBr pellets over the range of  $4000\text{--}400 \text{ cm}^{-1}$  on a NICOLET FT-IR NEXUS 670 spectrometer. The ultraviolet spectra (UV) were recorded on a SHIMADZU UV-Vis 1601PC spectrometer. The thermogravimetric analyses (TGA) were carried out using 19-20 mg samples and from 25 to  $500 \text{ }^\circ\text{C}$  with a  $5 \text{ }^\circ\text{C}/\text{min}^{-1}$  heating rate under a 50 ml/min dry nitrogen flux in a Mettler Toledo TGA/SDTA 851<sup>o</sup> thermal balance. The same equipment was used for differential scanning calorimetric (DSC) assays, but using 3.0-3.5 mg samples. The elemental analyses were carried out in duplicate in Perkin-Elmer 2400 and Eager 200 elemental analyzers with previously dried samples ( $45 \text{ }^\circ\text{C}$ , 24 h) with a reproducibility of  $\pm 0.3$ .

### 2.3. NMR Measurements

The solution phase NMR spectra were determined using a BRUKER AVANCE-400 spectrometer (400 MHz for  $^1\text{H}$  and 100 MHz for  $^{13}\text{C}$ ) and in a VARIAN UNITY-300 spectrometer (300 MHz for  $^1\text{H}$ , 75 MHz for  $^{13}\text{C}$  and 66.5 MHz for  $^{113}\text{Cd}$ ) using 5-mm sample tubes and  $\text{DMSO-}d_6$  (99.9 % D, CIL) as solvent.  $^1\text{H}$  and  $^{13}\text{C}$  chemical shifts were measured using the DMSO signal as an internal reference. The  $^{113}\text{Cd}$  chemical shifts were determined using a 1.0 M solution of  $\text{CdSO}_4$  in  $\text{D}_2\text{O}$  ( $\delta \text{ }^{113}\text{Cd}$  1.1 ppm) as an external reference. The solid state NMR spectra were determined using 250-mg samples packed in 7-mm zirconium rotors and a VARIAN INOVA 300 spectrometer with cross polarization and magic-angle spinning (CP/MAS). The  $^{13}\text{C}$  CP/MAS analyses were obtained with a spectral window of 50 kHz using a  $90^\circ$  pulse of 6  $\mu\text{s}$  and a relaxation delay of 3 s. Non-selective  $T_1$  values were measured using the standard inversion-recovery program. For the selective experiments using a BRUKER AVANCE-400 spectrometer, the  $180^\circ$  selective inversion pulse was achieved with a Gaussian selective pulse. For the selective experiments in the VARIAN UNITY-300 spectrometer, the  $180^\circ$ -selective inversion pulse was achieved by replacement of the hard  $180^\circ$ -pulse of the inversion-recovery sequence by a DANTE train (100 pulses,  $\tau = 40 \mu\text{s}$ ) with the transmitter power attenuation adjusted to 40 dB (19-dB attenuation in relation to the nonselective pulse). For the  $T_1$  NULL sequence [14-16], a selective  $180^\circ$ -pulse was located before the non-selective  $180^\circ$ -pulse from the standard inversion-recovery program and set in a VARIAN UNITY-300 spectrometer. The selective  $180^\circ$ -pulse was obtained using the composite pulse,  $\pi / 2_x - \pi_y - \pi / 2_x$ , in which each part was made up of a DANTE sequence (40 pulses,  $\tau = 40\text{--}50 \mu\text{s}$ ). This method gave better selectivity than a single  $180^\circ$ -DANTE pulse train. When the NULL sequence was used in the BRUKER spectrometer, the selective  $180^\circ$ -pulse was obtained by a Gaussian-shaped selective pulse.

### 2.4. Synthesis of $\text{Zn}(\text{DHA})_2(\text{py})$

A solution of 0.60 g (1.3 mmol) of  $\text{Zn}(\text{DHA})_2(\text{H}_2\text{O})_2$  in 3 ml of pyridine was refluxed over three hours. The excess of pyridine was evaporated under a vacuum, and the oily residue was poured on cold water to form a yellow solid, which was washed with water and acetone to produce pure 4 as white crystals in 85% yield. M.p.  $197\text{--}199 \text{ }^\circ\text{C}$

(dec.). Elemental Analysis Calculated for  $C_{21}H_{19}NO_8Zn$  (478.76g/mol): C, 52.68; H, 4.00; N, 2.93; O, 26.73. Found: C, 52.61; H, 3.73; N, 2.83. IR (KBr; pellet)  $\nu_{max}$  3078, 2996, 2929, 1697, 1654, 1590, 1494, 1427, 1403, 1342, 1244, 1163, 1126, 1065, 1010, 943, 842, 766, 573 and 525  $cm^{-1}$ . UV (MeOH):  $\lambda_{max}$  (nm) 291.20 ( $\epsilon = 0.262$ ), 262.40 nm ( $\epsilon = 0.178$ ), 256.20 nm ( $\epsilon = 0.171$ ), 230.80 nm ( $\epsilon = 0.420$ ).  $^1H$  NMR (400 MHz, DMSO- $d_6$ ):  $\delta$  8.57 (dd,  $J = 5.9$  and 1.7 Hz, 2H, H10); 7.79 (tt,  $J = 7.6$  and 1.7 Hz, 2H, H12); 7.39 (dd,  $J = 5.8$  and 1.8 Hz, H11); 5.63 (s, 2H, H5); 2.35 (s, 6H, H8); 2.05 (s, 6H, H9).  $^{13}C$  NMR (100 MHz, DMSO- $d_6$ ): 199.8 (C7); 182.7 (C4); 164.5 (C6); 162.3 (C2); 149.5 (C10); 136.2 (C12); 123.9 (C11); 107.5 (C5); 101.9 (C3); 32.1 (C8); 19.1 (C9).  $^{13}C$  NMR (CP/MAS)  $\delta$ : 202.2 (C7); 186.0 (C4); 164.9 (C6); 164.2 (C2); 150.1 (C10); 140.5 (C12); 124.7 (C11); 107.0 (C5); 101.2 (C3); 32.6 (C8); 19.4 (C9).

## 2.5. Synthesis of $Zn(DHA)_2(\gamma\text{-pic})$

A solution of 0.55 g (1.3 mmol) of  $Zn(DHA)_2(H_2O)_2$  in 3 ml of  $\gamma$ -picoline was refluxed over three hours. The excess of picoline was evaporated under a vacuum, and the residue was poured onto cold water to give a white solid, which was washed with acetone to yield pure **5** as a lightly yellow amorphous solid with 95% yield. M.p. 143.0-144.8°C (dec.). Elemental Anal. Calc. for  $C_{22}H_{21}NO_8Zn$  (492.78g/mol): C, 51.17; H, 4.30; N, 2.84; O, 25.97. Found: C, 50.1; H, 4.5; N, 2.7. IR (KBr; pellets)  $\nu_{max}$  3087, 3068, 3004, 2924, 1716, 1662, 1599, 811, 573  $cm^{-1}$ . UV (MeOH):  $\lambda_{max}$  (nm) 291.20 ( $\epsilon = 0.2621$ ), 262.40 ( $\epsilon = 0.1779$ ), 256.20 ( $\epsilon = 0.1713$ ), 230.80 ( $\epsilon = 0.4200$ ).  $^1H$  NMR (400 MHz, DMSO- $d_6$ ): 8.41 (d,  $J = 6.1$  Hz, 2H, H10); 7.22 (d,  $J = 5.0$  Hz, 2H, H11); 5.66 (s, 2H, H5); 2.36 (s, 6H, H13); 2.31 (s, 6H, H8); 2.05 (s, 6H, H9).  $^{13}C$  NMR (100 MHz, DMSO- $d_6$ ): 200.1 (C7); 182.9 (C4); 164.5 (C6); 162.5 (C2); 149.1 (C10); 147.1 (C12); 124.7 (C11); 107.5 (C5); 101.9 (C3); 32.1 (C8); 20.4 (C13); 19.1 (C9).

## 2.6. Synthesis of $Cd(DHA)_2(py)_2$

A solution of 0.55 g (1.3 mmol) of  $Cd(DHA)_2(H_2O)_2$  in 3 ml of pyridine was refluxed over three hours. The excess of pyridine was evaporated under a vacuum, and the oily residue poured into cold water to form a lightly yellow solid, which was washed with water to produce pure **6** as yellow crystals in 73 % yield. M.p.171-177 °C (dec.). Elemental Anal. Calc. for  $C_{26}H_{24}N_2O_8Cd$  (604.89 g/mol): C, 51.62; H, 4.01; N, 4.63; O, 21.16. Found: C, 51.6; H, 4.1; N, 22.3. IR (KBr, pellets)  $\nu_{max}$ , 3390, 3006, 2658, 1746, 1700, 1589, 1487, 1407, 1245, 1160, 1055, 1004, 925, 840, 760, 707, 622, 556, 517  $cm^{-1}$ . UV (MeOH): 293.60 nm ( $\epsilon = 0.217$ ), 262.20 nm ( $\epsilon = 0.106$ ), 255.60 nm ( $\epsilon = 0.115$ ), 230.80 nm ( $\epsilon = 0.425$ ).  $^1H$  RMN (400 MHz, DMSO- $d_6$ ): 8.56 (dd,  $J = 4.8$  and 1.6 Hz, 4H, H10); 7.79 (tt,  $J = 1.5$  and 7.8 Hz, H12); 7.39 (d,  $J = 4.8$  Hz, 4H, H11); 5.61 (s, 2H, H5); 2.35 (s, 6H, H8); 2.03 (s, 6H, H9).  $^{13}C$  RMN (100 MHz, DMSO- $d_6$ ): 201.2 (C7); 183.6 (C4); 164.9 (C6); 161.8 (C2); 149.6 (C10); 136.5 (C12); 124.1 (C11); 108.1 (C3); 102.7 (C5); 32.8 (C8) 19.2 (C9).  $^{13}C$  RMN (CP/MAS)  $\delta$ : 203.0 (C7); 186.0 (C4); 164.3 (C6); 163.3 (C2); 149.1(C10); 139.8(C12); 125.8 (C11); 107.7 (C3); 103.6(C5); 34.3(C8); 18.6 (C9).  $^{113}Cd$  RMN (66.5 MHz, DMSO- $d_6$ ): -10.4 (s).  $^{113}Cd$  RMN (CP/MAS): 39.4 (quint.,  $^1J_{Cd-N} = 126$  Hz).

## 2.7. Synthesis of $Cd(DHA)_2(\gamma\text{-pic})_2$

A solution of 0.55 g (1.3 mmol) of  $Cd(DHA)_2(H_2O)_2$  in 3 ml of  $\gamma$ -picoline was refluxed over three hours. The excess pyridine was evaporated under a vacuum, and the oily residue poured into cold water to form a white solid, which was washed with water to produce **7** as a yellow amorphous solid in 87 % yield. M.p.167-168 °C (dec.). Elemental Anal. Calc. for  $C_{28}H_{28}N_2O_8Cd$  (632.94 g/mol): C, 53.12; H, 4.47; N, 4.42; O, 20.22. Found: C, 53.1; H, 4.4; N, 4.5. IR (KBr, pellets)  $\nu_{max}$  3074, 2983, 2925, 2480, 1712, 1661, 1593, 954, 529  $cm^{-1}$ . UV (MeOH):  $\lambda_{max}$  (nm) 293.60 ( $\epsilon = 0.2175$ ), 262.20 ( $\epsilon = 0.1056$ ), 255.60 ( $\epsilon = 0.1155$ ), 230.80 ( $\epsilon = 0.4246$ ).  $^1H$  RMN (400 MHz, DMSO- $d_6$ ): 8.42 (dd,  $J = 4.8$  and 1.6 Hz, 4H, H10); 7.22 (d,  $J = 4.8$  Hz, 4H, H11); 5.60 (s, 2H, H5); 2.35 (s, 6H, H13); 2.31 (s, 6H, H8); 2.03 (s, 6H, H9).  $^{13}C$  RMN (100 MHz, DMSO- $d_6$ ): 204.1 (C7); 185.0 (C4); 166.7 (C6); 162.1 (C2); 150.6 (C10); 149.3 (C12); 125.9 (C11); 108.0 (C3); 103.9 (C5); 33.4 (C8); 21.6 (C13); 19.9 (C9).  $^{113}Cd$  RMN (66.5 MHz, DMSO- $d_6$ )  $\delta$ : -4.8 (s)

## 2.8. Molecular Modeling

The structures of the complexes were calculated and optimized using the Hartree-Fock and DFT B3LYP methods with the 3-21G, 6-31G\*\* and 6-31+G\* basis sets, as well as with the semiempirical method PM3: all employing the Spartan'06<sup>®</sup> program (Wavefunction, Inc.).

## 3. Results and Discussion

The synthesis of the complexes of DHA with Zn (**2**) and Cd (**3**) were previously reported by Chalaça, *et al.* [15] and Samus [17]. The zinc complexes **4** and **5** were obtained by direct reaction of complex **2** with pyridine (py) and  $\gamma$ -picoline (pic), respectively, in reflux for three hours. The elemental analyses for the zinc complexes **4** and **5** suggest that the structure of both possesses two DHA ligands and nitrogen aromatic ring ligands, indicating that complexes **4** and **5** are pentacoordinated. In order to study the nature of these two complexes, thermogravimetric analyses (TGA) were performed. Upon heating, complex **4** suffered degradation at 197-200 °C, and complex **5** degraded at 171-177 °C. The TGA of the Zn complexes **4** and **5** showed a mass loss of 17 and 19 %, respectively, corresponding to the loss of a single pyridine molecule around 194°C for compound **4** and a single  $\gamma$ -picoline molecule at 170°C for compound **5**. We then carried out a differential scanning calorimetric (DSC) assay, in which complex **4** showed two endothermic transformations: one at 209°C (-33.94 Kcal/kg<sup>-1</sup>), corresponding to the pyridine loss and other at 270°C

corresponding to its degradation. The DSC analysis of complex **5** showed only one endothermic transformation between 146 and 154°C ( $\approx -24.1 \text{ Kcal Kg}^{-1}$ ). Interestingly, no mass loss corresponding to water or other ligands was observed for either complex.

A similar set of reactions was carried out using cadmium as the metallic cation. The reaction of the  $\text{Cd}(\text{DHA})_2(\text{H}_2\text{O})_2$  (**3**) with the same ligands used for zinc complexes efficiently led to  $\text{Cd}(\text{DHA})_2(\text{py})_2$  (**6**) and  $\text{Cd}(\text{DHA})_2(\gamma\text{-pic})_2$  (**7**) (Scheme 1). The elemental analyses for the cadmium complexes **6** and **7** showed that these complexes possess two DHA ligands and two nitrogen aromatic ring ligands, which correspond to the hexacoordinated compounds.

These compounds do not display the same behavior of their corresponding zinc analogues on thermal analysis. For example, the TGA analysis of complex **7** showed a mass loss (10%) at 135-160 °C, corresponding to the loss of two  $\gamma$ -picoline molecules. Also, the DSC shows an endothermic transition between 135 and 169 °C ( $-28.2 \text{ Kcal Kg}^{-1}$ ) that corresponds to the loss of the two  $\gamma$ -picoline ligands. These results indicate that complex **7** is hexacoordinated.

Table 1 reports the selected vibrational bands of the ligands and their complexes. The bands of complexes **2** and **3** in the region  $3600\text{-}3100 \text{ cm}^{-1}$  are usually attributed to  $\nu(\text{OH})$ -stretching frequencies. These bands completely disappear in complexes **4-7** as a result of the complete substitution of the water ligands.

The comparison of the vibrational O-H stretching bands of dehydroacetic acid shows a considerable decrease in wave number ( $\sim 320\text{-}280 \text{ cm}^{-1}$ ) with respect to the corresponding free ligands as a consequence of the coordination with the cations. On the other hand, the vibrational modes of the C=O group do not show significant shifts with respect to the free ligand. The bands arising from the C-C and C=N bonds of the free ligands (pyridine and  $\gamma$ -picoline) undergo changes in frequency and intensity caused by the complexation. Also, in all the complexes, a medium band observed at  $580\text{-}515 \text{ cm}^{-1}$  can be attributed to the  $\nu(\text{M-N})$  and  $\nu(\text{M-O})$  vibration modes [18, 19].

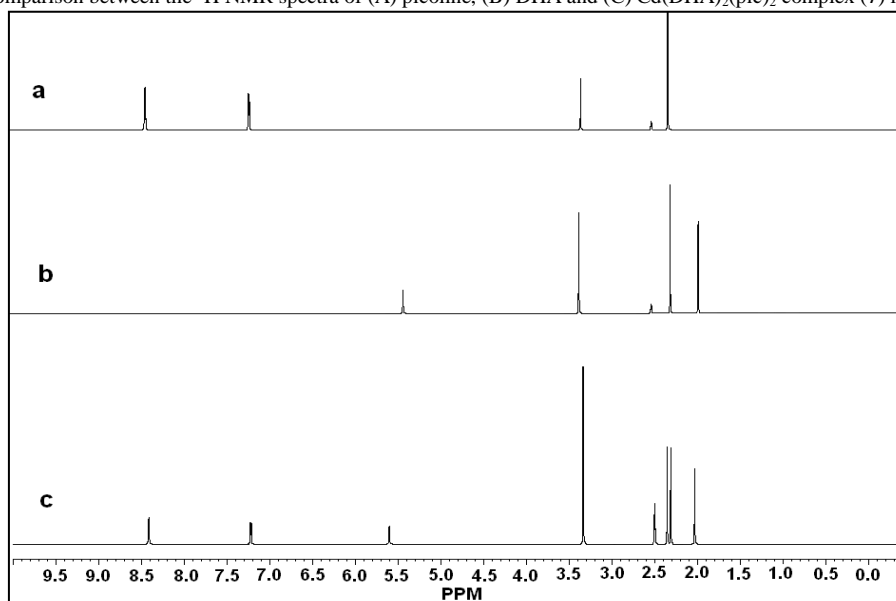
Table-1. IR frequencies,  $\nu$  ( $\text{cm}^{-1}$ ) of the free ligands and  $\text{Zn}^{2+}$  (**4**), (**5**) and  $\text{Cd}^{2+}$  (**6**), (**7**) complexes

Group	Pyridine	Picoline	DHA	4	5	6	7
C=O (C7)	--	--	1652	1655	1662	1660	1660
OH	--	--	3291	3079	3004	3080	2974
C-C	1437	1609	1570	1583	1599	1583	1590
C=N	1580	1416	--	1590	1416	1589	1416
M-O*	--	--	--	573	573	517	529

\* M =  $\text{Zn}^{2+}$  or  $\text{Cd}^{2+}$

Complexes **4-7** were also analyzed by NMR spectroscopy in  $\text{DMSO-}d_6$ . The intensity of the  $^1\text{H}$  NMR of the complexes showed that the entity formed includes two DHA molecules for all complexes, but only one pyridine or one  $\gamma$ -picoline molecule for complexes **4** and **5**, respectively. Nevertheless, two pyridines and two  $\gamma$ -picoline ligands were present in complexes **6** and **7**, confirming the assumed octahedral geometry for the Cd complexes. The NMR results showed that the chemical shifts for pyridine and  $\gamma$ -picoline are almost identical in the free and bound forms, which is not the case for DHA, as shown in Figure 1.

Fig-1. Comparison between the  $^1\text{H}$  NMR spectra of (A) picoline, (B) DHA and (C)  $\text{Cd}(\text{DHA})_2(\text{pic})_2$  complex (**7**) in  $\text{DMSO-}d_6$



In the  $^1\text{H}$  NMR spectra of complexes **5** and **7**, the signals for H5, H8, H9 and H13 are shifted downfield while the signals for H10 and H11 had no observed shifts (Table 2). The most substantial changes in chemical shifts were observed for the H5 of complexes **4-7**, in which the signals were shifted downfield approximately 0.27 ppm. On the other hand, the  $J_{\text{H,H}}$  coupling constants (see the data from the Experimental section) for the free  $\gamma$ -picoline ligand, when compared to complexes **4** and **5**, remain basically unaffected by the complexation.

**Table-2.** Chemical shifts (ppm) of different hydrogens of pure DHA, pyridine,  $\gamma$ -picoline and their complexes in DMSO- $d_6$ 

Compound	H5	H8	H9	H10	H11	H12	H13
DHA	5.39 (1H)	2.27 (3H)	1.95 (3H)	-	-	-	-
Py	-	-	-	8.57 (2H)	7.37 (2H)	7.77(1H)	-
Pic	-	-	-	8.42 (2H)	7.21 (2H)	-	2.31(3H)
4	5.63 (2H)	2.35 (6H)	2.05(6H)	8.57(2H)	7.39 (2H)	7.79(1H)	-
5	5.66 (2H)	2.31 (6H)	2.05 (6H)	8.41 (2H)	7.22 (2H)	-	2.36 (3H)
6	5.61 (2H)	2.36 (6H)	2.03 (6H)	8.57(4H)	7.39(4H)	7.79(2H)	-
7	5.60 (2H)	2.31 (6H)	2.03 (6H)	8.42 (4H)	7.22 (4H)	-	2.35 (6H)

Investigation of compounds **4-7** by  $^{13}\text{C}$  NMR spectroscopy provided the most detailed information on the structure of these complexes. The results are summarized in **Table 3**. Interestingly, upon complex formation, DHA suffered a more significant chemical shift variation than the other two ligands (pyridine and  $\gamma$ -picoline). Due to complexation, DHA was observed to be unshielding in all complexes. Regarding the changes in ligand chemical shifts upon complexation, the most significant variations were observed for carbon C7 as well as for C4, the carbonyl carbon of DHA. These changes can be easily explained by the complexation process. For all of these carbons, complexation leads to a decrease in electron density due the carbonyl oxygen are involved in bonding with the metal. For C7 and C4, the greatest change ( $\Delta\delta$ ) are observed for the picoline complex with Cd (**7**), corresponding to 4.7 ppm and 2.7 ppm, respectively.

**Table-3.**  $^{13}\text{C}$  NMR chemical shifts for DHA, picoline and for the complexes in solution

Compound	Pyridine	Picoline	DHA	4	5	6	7
C <sub>2</sub>	--	--	158.9	162.3	162.5	161.8	161.7
C <sub>3</sub>	--	--	102.2	101.9	101.9	102.7	102.6
C <sub>4</sub>	--	--	180.7	182.7	182.9	183.6	183.4
C <sub>5</sub>	--	--	109.0	107.5	107.5	108.1	108.0
C <sub>6</sub>	--	--	163.5	164.5	164.5	164.9	164.7
C <sub>7</sub>	--	--	196.2	199.8	200.1	201.2	200.9
C <sub>8</sub>	--	--	32.1	32.1	32.1	32.8	32.7
C <sub>9</sub>	--	--	19.2	19.1	19.1	19.2	19.1
C <sub>10</sub>	150.2	149.3	--	149.5	149.1	149.6	149.3
C <sub>11</sub>	123.9	124.3	--	123.9	124.7	124.1	124.7
C <sub>12</sub>	135.9	146.6	--	136.2	147.1	136.5	146.9
C <sub>13</sub>	--	19.9	--	--	20.4	--	20.4

The  $^{113}\text{Cd}$  NMR spectrum of complex **3** showed a single signal at -18.5 ppm, which is a strong indication that Cd is coordinated to six oxygen atoms, as reported by [Chalçaça, et al. \[15\]](#). Complexes **6** and **7** showed  $^{113}\text{Cd}$  NMR signal at -10.4 and -4.8 ppm, respectively. These results confirm that the environment of the Cd cation changes due to coordination with nitrogen atoms, which is in agreement with the literature [20-22].

Further evidence for the complex formation is the existence of intramolecular nOe between the H5 of DHA and the H10 of picoline. Saturation of H5 produces nOe enhancement at H10 in complexes **5** and **7**.

Measurement of  $^1\text{H}$  spin-lattice relaxation times was carried out in diluted solutions of DMSO- $d_6$  with DHA,  $\gamma$ -picoline, pyridine and complexes **4-7**. For all complexes, the results demonstrated that  $T_1$  decreases when compared to the  $T_1$  values for the free ligands. Even greater changes were observed for  $\gamma$ -picoline (**Table 4**).

**Table-4.** Non-selective (NS) spin-lattice relaxation measurements (s) for 0.2 M solutions of the free and complexed ligands

Hydrogen	Picoline	Pyridine	DHA	4	6	5	7
H5	--	--	3.88	3.01	3.24	3.06	2.17
H8	--	--	1.37	0.88	0.97	1.16	0.86
H9	--	--	0.99	0.81	0.82	0.77	0.81
H10	9.37	10.02	--	8.43	8.25	5.34	1.54
H11	7.54	11.52	--	8.05	7.62	4.95	1.72
H12	--	9.10	--	8.92	8.39	--	--
H13	4.22	--	--	--	1.04	--	0.85

In order to obtain information on the geometry of the complexes in solution, we carried out experimental measurements of the distance between the olefinic hydrogen (H5) and the H<sub>ortho</sub> of  $\gamma$ -picoline (H10) using the NULL method [14-16, 23, 24]. NULL allows a precise determination of interproton distances when compared to methods based on nOe [25, 26] because it minimizes spin diffusion effects. The NULL pulse sequence starts with a selective composite  $180^\circ$ -hydrogen pulse, which inverts the magnetization of only the hydrogen of interest for the desired distance determination. In the present case, it was decided to selectively invert H5. The NULL experiment continues with a non-selective  $180^\circ$ -pulse, which resets the selected hydrogen magnetization back to the +z-axis while inverting all other hydrogens to the -z axis. The experiment continues with a variable time period followed by a  $90^\circ$ -

pulse and detection, thus allowing for the determination of the longitudinal relaxation times of all hydrogens without their cross-relaxation with the initially selected hydrogen.

If the molecular correlation time ( $\tau_c$ ) is known, it is possible to use the cross-relaxation value to calculate the distance between the selectively excited hydrogen ( $H_i$ ) with any one of the other hydrogens ( $H_j$ ), as shown in Equation 1 [14-16, 25, 27-31] where  $\rho_{ij}$  is the cross relaxation term for  $H_i$  and  $H_j$ .

$$r_{ij} = \left[ \frac{3}{8} \left( \frac{\mu_o}{4\pi} \right)^2 \frac{\gamma^4 h \tau_c}{4\pi \rho_{ij}} \right]^{1/6} \quad \text{Equation 1}$$

In this work, the correlation time ( $\tau_c$ ) was calculated by carrying out determinations for selective and nonselective  $T_1$ , and these results were used for the correlation of  $R_1^S/R_1^{NS}$  with  $\omega\tau_c$  [27, 28, 32].

The NULL method allows for the experimental determination of H-H distances in solution with a precision of  $\pm 0.01$  Å. The results of this study are shown in Table 5.

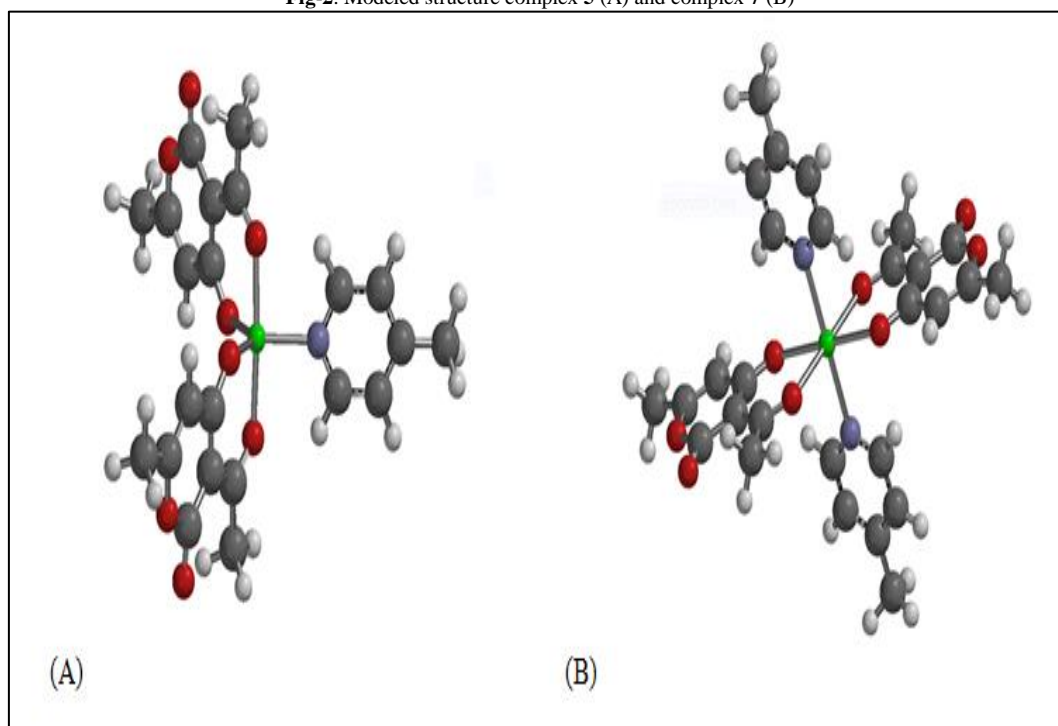
In order to compare the experimental H-H distances obtained with NULL with calculated data, a molecular modeling study of these molecules was carried out using the Spartan'06 program [33]. The calculations for comparison were conducted using a 3-21G basis set because the use of more complex basis sets could not be performed with the Cd complexes using this program. However, some calculations with Zn complexes were performed using both the Hartree-Fock and B3LYP methods with the basis sets 3-21G, 6-31G\*\* and 6-31+G\*; the results were quite similar, indicating that the use of the 3-21G was convenient for the comparison of geometries. The structure calculations for all the complexes were also performed using the semiempirical method of PM3. The pentacoordinated Zn complexes could, in principle, possess two possible structures: trigonal bipyramidal geometry or square pyramidal geometry. All the calculations for the Zn complexes with pentacoordination, even when starting with a square pyramidal geometry, led to bipyramidal structures. In addition, these structures always have the pyridine or picoline ligands located at the trigonal plane, as shown in Figure 2. It was also found that the lowest energy for the different bipyramidal complexes was the structure with the acetyl carbonyl groups of the dehydroacetic acid ligands located at the two axial positions. However, the energy differences between all the possible bipyramidal complexes varied from 0.43 to 0.71 kcal/mol, which is quite small. The molecular modeling calculation results of the distance between the dehydroacetic acid vinyl hydrogen (H5) and the *ortho*-hydrogens of the pyridine or picoline ligands (H10) were determined for the lowest energy complexes and are shown in Table 5, corresponding to an average of all the H5-H10 distances for each complex. It is important to make clear that the H5-H10 distance is very similar between all the possible bipyramidal Zn complexes.

**Table-5.** Calculated and Experimental H-5 and H-10 distances for all complexes

		DFT	PM3
4	5.49	5.82 <sup>a</sup>	4.77
5	4.98	5.83 <sup>a</sup>	4.77
6	4.55	3.66 <sup>b</sup>	3.80
7	4.29	3.67 <sup>b</sup>	3.67

<sup>a</sup>Calculated with the basis set 6-31+G\*. <sup>b</sup>Calculated with the basis set 3-21G

**Fig-2.** Modeled structure complex 5 (A) and complex 7 (B)



Despite the inexistence of the octahedral complexes  $\text{Zn}(\text{DHA})_2(\text{py})_2$  and  $\text{Zn}(\text{DHA})_2(\gamma\text{-pic})_2$ , we studied them by molecular modeling in order to compare their potential structural data with the respective bipyramidal complexes [2, 34-36]. The modeling of octahedral Zn complexes indicated that their H5-H10 distances correspond to 3.765 Å, which is approximately 35% shorter than the calculated value for the bipyramidal complexes (5.83 Å). The experimental H5-H10 distances for the octahedral Cd complexes observed were 4.55 and 4.29 Å, as shown in Table 5. These values, despite being referent to the complexes of a greater cation, are shorter than the experimental values for the Zn complexes (5.49 and 4.98 Å). These result that agrees with the molecular modeling results. These results confirm the trigonal bipyramidal geometry with the pyridine or picoline ligand out of the axial positions for pentacoordinated Zn complexes 4 and 5. From Table 5, it is also apparent that the numbers of the calculated H-H distances do not correspond precisely with the experimental data, but their relative values certainly confirm the proposed geometry for all the compounds.

It is also important to notice that the experimental H5-H10 distances calculated with the NULL method are shorter for complexes 5 and 7, in agreement with the fact that picoline is a stronger ligand than pyridine [37, 38]. However, the results obtained by molecular modeling with B3LYP do not detect that difference, and the PM3 results display that difference only for the Cd complexes.

## 4. Conclusion

Water-dehydroacetic acid complexes of Zn and Cd are good starting materials for the synthesis of several new coordination compounds by substituting water with other ligands, like DMSO, pyridine and picoline. This quite efficient procedure leads to very good yields.

The structural characterization of the final complexes clearly showed that the Cd complexes are octahedral, while the Zn complexes are bipyramidal trigonal with the pyridine or picoline ligand not localized at the axial position. These results indicate that the substitution of Zn by Cd in the study of Zn-proteins or other coordination compounds has significant potential for important changes in the metal complexation geometry. Previously, it was shown that the exchange of water for weak ligands, like DMSO, differentiates the Cd and Zn complexes only with respect to the metal-ligand bond distances. However, this work confirms that greater changes in molecular geometry are observed when strong ligands, such as pyridine and picoline, are involved.

In this work, it was also shown that the NULL method is an important tool for the determination and comparison of the geometry of diamagnetic complexes in solution via the experimental determination of H-H distances.

## Acknowledgments

We are grateful to the following Brazilian agencies for financial support and fellowships: CNPq, CAPES, INCT-CNPq (IMBEBB) and FAPERJ. We also thank P. P. P. Netto, D. A. P. da Mota e C. H. B. Bizarri for their help on the acquisition of some spectroscopy data.

## References

- [1] Kasampalidis, I. N., Pitas, I., and Lyroudia, K. K., 2007. "Conservation of metal-coordinating residues." *Proteins Structure Function Bioinformatics*, vol. 68, p. 123.
- [2] Pal, R., Kumar, V., Gupta, A. K., and Beniwal, V., 2014. "Synthesis, characterization and DNA photocleavage study of a novel dehydroacetic acid based hydrazone schiff's base and its metal complexes." *Medicinal Chemistry Research*, vol. 23, pp. 3327–3335.
- [3] Barszcz, B., Jablonska-Wawrzycha, A., Stadnicka, K., and Hodorowicz, S. A., 2005. "The synthesis and structural characterization of novel zinc and cadmium complexes of chelating alcohol." *Inorganic Chemistry Communications*, vol. 8, pp. 951-954.
- [4] Hall, M. D. and Hambley, T. W., 2002. "Platinum(IV) antitumor compounds: their bioinorganic chemistry." *Coordination Chemistry Reviews*, vol. 232, pp. 49-67.
- [5] Farrell, N., 2002. "Biomedical uses and applications of inorganic chemistry. An overview." *Coordination Chemistry Reviews*, vol. 232, pp. 1-4.
- [6] Parkin, G., 2004. "Synthetic analogues relevant to the structure and function of zinc enzymes." *Chemical Review*, vol. 104, pp. 699-768.
- [7] Roohani, N., Hurrell, R., Kelishadi, R., and Schulin, R., 2013. "Zinc and its importance for human health: An integrative review." *Journal of Research in Medical Sciences*, vol. 18, pp. 144–157.
- [8] Das, J. K., Khan, R. S., and Bhutta, Z. A., 2018. *Chapter 21 - zinc fortification, food fortification in a globalized world*. Academic Press, pp. 213-219.
- [9] Soisungwan, S., Scott, G. H., Sens, M., and Sens, D. A., 2011. "Cadmium, environmental exposure, and health outcomes." *Ciência and Saúde Coletiva*, vol. 16, pp. 2587-2602.
- [10] Waalkes, M. P., 2000. "Cadmium carcinogenesis in review." *Journal of Inorganic Biochemistry*, vol. 79, pp. 241-244.
- [11] Kaakoush, N. O., Raftery, M., and Mendz, G. L., 2008. "Molecular responses of *Campylobacter jejuni* to cadmium stress." *The FEBS Journal*, vol. 275, pp. 5021-5033.
- [12] Iranzo, O., Jakusch, T., Lee, K. H., Hemmingsen, L., and Pecoraro, V. L., 2009. "The correlation of  $^{113}\text{Cd}$  NMR and  $^{111}\text{Cd}$  PAC spectroscopies provides a powerful approach for the characterization of the structure of Cd(II)-substituted Zn(II) proteins." *Chemistry*, vol. 15, pp. 3761-3772.

- [13] Kidambi, S. S., Lee, D. K., and Ramamoorthy, A., 2003. "Interaction of cd and zn with biologically important ligands characterized using solid-state nmr and ab initio calculations." *Inorganic Chemistry*, vol. 42, p. 3142.
- [14] Armitage, I. M., Drakenberg, T., and Reilly, B., 2013. "Use of 113Cd NMR to probe the native metal binding sites in metalloproteins: an overview." *Metal Ions in Life Sciences*, vol. 11, pp. 117-144.
- [15] Chalaça, M. Z., Figueroa-Villar, J. D., Ellena, J. A., and Castellano, E. E., 2002. "Synthesis and structure of cadmium and zinc complexes of dehydroacetic acid." *Inorganica Chimica Acta*, vol. 328, pp. 45-52.
- [16] Carvalho, E. M., Figueroa-Villar, J. D., Greco, S. J., Pinheiro, S., and Carneiro, J. W. M., 2007. "Conformational characterization of a camphor-based chiral  $\gamma$ -amino alcohol." *Journal of Molecular Structure*, vol. 827, pp. 1-3.
- [17] Carvalho, E. M., Velloso, M. H. R., Tinoco, L. W., and Figueroa-Villar, J. D., 2003. "Formation of p-cresol: piperazine complex in solution monitored by spin-lattice relaxation times and pulsed field gradient NMR diffusion measurements." *Journal of Magnetic Resonance*, vol. 164, pp. 197-204.
- [18] Ouari, K., Bendia, S., Weiss, J., and Bailly, C., 2015. "Spectroscopic, crystal structural and electrochemical studies of zinc(ii)-schiff base complex obtained from 2,3-diaminobenzene and 2-hydroxy naphthaldehyde. Spectrochimica acta part A." *Molecular and Biomolecular Spectroscopy*, vol. 135, pp. 624-631.
- [19] Hazra, M., Dolai, T., Giri, S., Patra, A., and Dey, S. K., 2017. "Synthesis of biologically active cadmium (II) complex with tridentate N2O donor Schiff base: DFT study, binding mechanism of serum albumins (bovine, human) and fluorescent nanowires." *Journal of Saudi Chemical Society*, vol. 21, pp. S445-S456.
- [20] Thornton, D. A., 1990. "Infrared spectra of metal  $\beta$ -ketoenolates and related complexes." *Coordination Chemistry Reviews*, vol. 104, pp. 173-249.
- [21] Bennett, A. M. A., Foulds, G. A., and Thornton, D. A., 1989. "The IR and 1H, 13C NMR spectra of the nickel(II), copper(II) and zinc(II) complexes of 2,4-pentanedione, 4-imino-2-pentanone, 4-thioxo-2-pentanone and 2,4-pentanedithione: a comparative study." *Polyhedron*, vol. 8, pp. 2305-2311.
- [22] Summers, M. F., 1988. "113Cd NMR spectroscopy of coordination compounds and proteins." *Coordination Chemistry Reviews*, vol. 86, pp. 43-134.
- [23] Lipton, A. S., Mason, S. S., Reger, D. L., and Ellis, P. D., 1994. "113cd shielding tensors of monomeric cadmium compounds containing nitrogen donor atoms. 1. Cp/mas studies on cadmium poly(pyrazolyl)borate complexes having n4 and n6 coordination environments." *Journal of the American Chemical Society*, vol. 116, pp. 10182-10187.
- [24] Ma, G., Fischer, A., Nieuwendaal, R., Ramaswamy, K., and Hayes, S. E., 2005. "Cd(II)-ethylenediamine mono- and bimetallic complexes. Synthesis and characterization by 113Cd NMR spectroscopy and single crystal X-ray diffraction." *Inorganica Chimica Acta*, vol. 358, pp. 3165-3173.
- [25] Neuhaus and Williamson, M. P., 2000. *The nuclear overhauser effect in structural and conformational analysis*. 2nd ed. New York: Wiley-VCH.
- [26] Tarafder, M. T. H., Jin, K. T., Crouse, K. A., Ali, A. M., Yamin, B. M., and Fun, H. K., 2002. "Coordination chemistry and bioactivity of Ni<sup>2+</sup>, Cu<sup>2+</sup>, Cd<sup>2+</sup> and Zn<sup>2+</sup> complexes containing bidentate Schiff bases derived from S-benzylthiocarbamate and the X-ray crystal structure of bis[S-benzyl- $\beta$ -N-(5-methyl-2-furylmethylene)dithiocarbamate]cadmium(II)." *Polyhedron*, vol. 21, pp. 2547-2554.
- [27] Brand, T., Cabrita, E. J., and Berger, S., 2005. "Intermolecular interaction as investigated by NOE and diffusion studies." *Progress in Nuclear Magnetic Resonance Spectroscopy*, vol. 46, pp. 159-196.
- [28] Tinoco, L. W. and Figueroa-Villar, J. D., 1999. "Determination of correlation times from selective and non-selective spin-lattice relaxation rates and their use in drug-drug and drug-albumin interaction studies." *Journal of the Brazilian Chemical Society*, vol. 10, pp. 281-286.
- [29] Hill, D. W. R., Tomlinson, B. L., and Hall, L. D., 1974. "Dipolar contribution to NMR spin-lattice relaxation of protons." *The Journal of Chemical Physics*, vol. 61, pp. 4466-4473.
- [30] Freeman, R., 1991. "Selective excitation in high-resolution NMR." *Chemical Review*, vol. 91, pp. 1397-1412.
- [31] Boros, S., Gáspári, Z., and Batta, G., 2018. "Accurate nmr determinations of proton-proton distances." *Annual Reports on NMR Spectroscopy*, vol. 94, pp. 1-39.
- [32] Neuhaus, 2000. *Williamson the nuclear overhauser effect in structural and conformational analysis*. 2nd ed. Wiley-VCH, Weinheim.
- [33] Shao, Y., Molnar, L. F., Jung, Y., Kussmann, J., Ochsenfeld, C., Brown, S. T., Gilbert, A. T. B., Slipchenko, L. V., Levchenko, S. V., et al., 2006. "Advances in methods and algorithms in a modern quantum chemistry program package." *Physical Chemistry Chemical Physics*, vol. 8, pp. 3172-3191.
- [34] Bouchama, A., Bendaás, A., Chiter, C., Beghidja, A., and Djedouani, A., 2007. "Bis(3-acetyl-6-methyl-2-oxo-2H-pyran-4-olato)bis(dimethylformamide)copper (II)." *Acta Crystallographica Section E*, vol. 63, p. m2397.
- [35] Djedouani, A., Bendaás, A., Bouacida, S., Beghidjac, A., and Douadia, T., 2006. "Bis[3-acetyl-6-methyl-2H-pyran-2,4(3H)-dionato] bis(dimethyl sulfoxide)copper(II)." *Acta Crystallographica Section E*, vol. 62, pp. m133-m135.
- [36] Zouchoune, F., Zendaoui, S., Bouchakri, N., Djedouani, A., and Zouchoune, B., 2010. "Electronic structure and vibrational frequencies in dehydroacetic acid (DHA) transition-metal complexes: A DFT study." *Journal of Molecular Structure: THEOCHEM*, vol. 94, pp. 78-84.



- [37] Audergon, L., Emmenegger, F., Piccand, M., Piekarski, H., and Mokrzan, J., 2001. "Comparison of pyridine and 4-methyl-pyridine as ligands to cobalt(II) chloride in the gas phase and in solution." *Polyhedron*, vol. 20, pp. 387-394.
- [38] Sutradhar, M., Mukherjee, G., Drew, M. G., and Ghosh, S., 2006. "Synthesis, reactivity, and x-ray crystal structure of some mixed-ligand oxovanadium(v) complexes: First report of binuclear oxovanadium(v) complexes containing 4,4'-bipyridine type bridge." *Inorganic Chemistry*, vol. 45, pp. 5150-5161.